

CLUSTER CHEMISTRY

XVI *. SYNTHESIS AND CRYSTAL STRUCTURE OF $\text{AuFe}_3(\mu_3\text{-HC=NBu}^t)(\text{CO})_9(\text{PPh}_3)$, AN AuFe_3 BUTTERFLY CLUSTER

MICHAEL I. BRUCE * and BRIAN K. NICHOLSON **

Jordan Laboratories, Department of Physical and Inorganic Chemistry, University of Adelaide, Adelaide, South Australia, 5001 (Australia)

(Received November 22nd, 1982)

Summary

The reaction between $\text{AuCl}(\text{PPh}_3)$ and $[\text{Fe}(\mu_3\text{-HC=NBu}^t)(\text{CO})_9]^-$ gives $\text{AuFe}_3(\mu_3\text{-HC=NBu}^t)(\text{CO})_9(\text{PPh}_3)$, crystals of which are triclinic, space group $P\bar{1}$, with a 12.815(3), b 16.265(4), c 19.106(3) Å, α 67.15(3), β 73.46(2), γ 73.12(2)° and $Z = 4$. The complex contains an AuFe_3 “butterfly” cluster, the Fe_3 face of which is bridged by the HC=NBu^t ligand bonded in the $(2\sigma + \pi)$ mode on the side opposite to the $\text{Au}(\text{PPh}_3)$ moiety, which, contrary to expectation based on the analogy with H, bridges the two Fe atoms σ -bonded to N, and π -bonded to the C=N group. The $\text{AuFe}_2/\text{Fe}_3$ dihedral angles in the two independent molecules differ significantly, with values of 110.9 and 132.1°.

Introduction

Although the first complexes containing transition metal–gold bonds were described nearly twenty years ago [1], the recent upsurge in interest in these compounds has been encouraged, in part, by the realisation that the $\text{Au}(\text{PR}_3)$ moiety is isolobal with H, and also by the finding by several groups that addition of several $\text{Au}(\text{PR}_3)$ groups to a transition metal cluster can occur. Thus, Lauher's demonstration that the $\text{Au}(\text{PPh}_3)$ group in $\text{AuCo}_3\text{Fe}(\text{CO})_{12}(\text{PPh}_3)$ occupies a similar Co_3 -face-bridging position to that of H in $\text{HCo}_3\text{Fe}(\text{CO})_{12}$ [2] was quickly followed by structural studies with other gold-containing clusters [3] and by a theoretical study rationalising these results [4]. Almost at the same time, reports of the syntheses of polygold clusters, such as $\text{Au}_3\text{V}(\text{CO})_5(\text{PPh}_3)_3$ [5], $\text{H}_2\text{Au}_2\text{Os}_4(\text{CO})_{12}(\text{PPh}_3)_2$ [6], and

* For Part XV, see ref. 26.

** On leave from the University of Waikato, Hamilton (New Zealand).

including seven-atom clusters with the then unprecedented tricapped tetrahedral core geometry, $\text{HAu}_3\text{Ru}_4(\text{CO})_{12}(\text{PPh}_3)_3$ [7,8] and $\text{Au}_3\text{CoRu}_3(\text{CO})_{12}(\text{PPh}_3)_3$ [8] began to appear.

Our work in this area, which began with the use of the gold-oxonium reagent $[\text{O}(\text{Au}(\text{PPh}_3))_3]^+$ [9] as a vehicle for the introduction of up to three gold atoms into metal cluster compounds, has recently been directed towards the synthesis of related compounds containing simple molecules, such as olefins, alkynes or isocyanides, attached to the metal cluster, with a view to studying changes in reactivity of these molecules as the size of the cluster is increased. At the same time, we hoped to obtain more information concerning the factors which cause the $\text{Au}(\text{PR}_3)$ moiety variously to cap the face of a cluster, as in the above-mentioned complexes, or to occupy edge-bridging sites, as found in $\text{H}_2\text{AuRu}_3(\mu_3\text{-COMe})(\text{CO})_9(\text{PPh}_3)$ [7]. The first results have been obtained with systems in which hydride has been added to the cluster-bonded ligand, such as $\text{HRu}_3(\mu_3\text{-C}_2\text{Bu}^i)(\text{CO})_9$, which on successive reactions with $\text{K}[\text{HB}(\text{CH}_2\text{CHMe}_2)_3]$ and $[\{\text{Au}(\text{PPh}_3)\}_3\text{O}]^+$ affords the *t*-butylvinylidene complex, $\text{Au}_2\text{Ru}_3(\mu_3\text{-C}=\text{CHBu}^i)(\text{CO})_9(\text{PPh}_3)_2$ [10]; the related reaction between $\text{Fe}_3(\mu_3\text{-CNBu}^i)(\text{CO})_9$ and $\text{AuCl}(\text{PPh}_3)$ is the subject of this paper.

We have recently described a high-yield, specific synthesis of $\text{Fe}_3(\mu_3\text{-CNBu}^i)(\text{CO})_9$ (I) which is readily reduced to $[\text{Fe}_3(\mu_3\text{-HC}=\text{NBu}^i)(\text{CO})_9]^-$ (II), subsequent protonation giving $\text{HFe}_3(\mu_3\text{-HC}=\text{NBu}^i)(\text{CO})_9$ (III) [11]. Ruthenium [12] and osmium [13] analogues of II and III are known and related iron complexes have also been prepared recently by less straightforward routes [14–16].

The orientational change of the cluster-bonded isocyanide with respect to the Fe_3 triangle in I and II is related to the parallel or perpendicular coordination of alkynes recently and comprehensively discussed by Schilling and Hoffmann [17]. This change can also be rationalised in terms of the skeletal electron-pair counting procedure of Wade [18]: thus I with 52 electrons approximates a *closo* trigonal bipyramid, while II with 54 electrons has a *nido* octahedral core. This approach leads to a prediction that it should be possible to cap the Fe_2CN face of II to give a *closo* octahedral core. However, no example of an $\text{Au}(\text{PR}_3)$ moiety capping a square face has been described to date; in $\text{Au}_2\text{Fe}_4\text{C}(\text{CO})_{12}(\text{PEt}_3)_2$, the gold atom is also bonded to the interstitial carbon atom [19].

Experimental

Reactions were carried out under an inert atmosphere (N_2) using standard Schlenk techniques. The preparation of $\text{Fe}_3(\mu_3\text{-CNBu}^i)(\text{CO})_9$ (I) has been detailed elsewhere [20].

Preparation of $\text{AuFe}_3(\mu_3\text{-HC}=\text{NBu}^i)(\text{CO})_9(\text{PPh}_3)$ (IV)

A solution of $\text{Fe}_3(\mu_3\text{-CNBu}^i)(\text{CO})_9$ (0.10 g, 0.20 mmol) in THF (10 cm^3) was treated with $\text{K}[\text{HBBu}_3]$ (0.45 cm^3 of a 0.5 mol l^{-1} solution in THF, 0.22 mmol). After 10 minutes, to the resulting solution of $[\text{Fe}_3(\mu_3\text{-HC}=\text{NBu}^i)(\text{CO})_9]^-$ was added solid $\text{AuCl}(\text{PPh}_3)$ (0.10 g, 0.20 mmol); TLC indicated a rapid reaction to give one purple product. After 30 minutes THF was removed and the residue extracted with Et_2O (50 cm^3). After filtration the extract was concentrated to ca. 15 cm^3 , an equal volume of petroleum ether (40–60°C) was added and the mixture cooled to -30°C to give black rosettes of the product IV (0.12 g, 63%). Found: C, 40.39; H, 2.42; N,

1.44%; $C_{32}H_{25}AuFe_3NO_9P$ calcd.: C, 39.91; H, 2.62; N, 1.45%. $\nu(CO)$ (CH_2Cl_2) 2054m, 2003vs, 1970s, 1950w(sh), 1932w(sh) cm^{-1} . 1H NMR: δ ($CDCl_3$) 10.00, s, $H-C=$; 7.57, m, C_6H_5 ; 1.29, s, $(CH_3)_3C$.

Crystal structure of $AuFe_3(\mu_3-HC=NBu^')(CO)_9(PPh_3)$ (IV)

An intensely-coloured deep-red prismatic crystal of dimensions $0.13 \times 0.11 \times 0.09$ mm was grown from CH_2Cl_2 /hexane solution and mounted on an Enraf-Nonius CAD4 diffractometer. Lattice parameters were determined using the setting angles of 25 high-angle reflections.

Crystal data. $C_{32}H_{25}AuFe_3NO_9P$, $M = 963.01$, triclinic, space group $P\bar{1}$, a 12.815(3), b 16.265(4), c 19.106(3) Å, α 67.15(2), β 73.46(2), γ 73.12(2)°, U 3444 Å³. D_m 1.85(1) $g\ cm^{-3}$, D_c 1.857 $g\ cm^{-3}$ for $Z = 4$. $F(000) = 1872$, $\mu(Mo-K\alpha)$ 55.45 cm^{-1} .

Intensity data were collected in the range $1.5^\circ < \theta < 20^\circ$ using an $\omega - \frac{n}{3}\theta$ scan where the optimum value of n was found to be 3 by an analysis of peak shape. Horizontal counter apertures and ω scan angles of $(2.40 + 0.80 \tan \theta)$ mm and $(0.08 + 0.35 \tan \theta)^\circ$ respectively were used. The data were corrected for Lorentz and polarisation effects (SUSCAD) and for absorption (ABSORB) [21]. Of the 5454 unique reflections collected, those 4128 with $I > 2.5 \sigma(I)$ were used in all calculations.

Solution and refinement. The two gold atoms in the asymmetric unit were located by Patterson methods and subsequent refinement cycles/difference maps revealed all other non-hydrogen atoms. In the final blocked full-matrix least-squares refinement cycles the metal and phosphorus atoms were treated anisotropically, the other atoms were assigned isotropic temperature factors, and the phenyl rings were treated as rigid groups ($d(C-C)$ 1.395 Å). Hydrogen atoms were not included. The refinement converged at $R = 0.042$, $R_w = 0.046$ where $w = 1.62 (\sigma^2(F_o) + 0.00038 F_o^2)^{-1}$ with no parameter shifting in the final cycle by more than 0.9 σ . A final difference map showed no peaks greater than 0.7 $e\ \text{\AA}^{-3}$. All calculations were performed using SHELX [21].

Final atomic positions are given in Table 1 and selected bond parameters in Table 2. Views of the two independent molecules are in Fig. 1, while the unit cell packing is shown in Fig. 2*.

Results and discussion

The reaction between $[Fe_3(\mu_3-HC=NBu^')(CO)_9]^-$ (II) and $AuCl(PPh_3)$ (Scheme 1) occurred readily giving one cluster product, $AuFe_3(\mu_3-HC=NBu^')(CO)_9(PPh_3)$ (IV), which forms air-stable crystals. Solutions of IV are moderately air-sensitive. The similarity of colour, and position of the $H-C=N$ 1H NMR resonance of those of $HFe_3(\mu_3-HC=NBu^')(CO)_9$ (III) suggested an edge-bridging position for the Au atom in IV but a full crystal structure analysis was undertaken to obtain details.

Structure of IV. The crystal consists of discrete molecules. The two independent molecules are approximate non-superimposable mirror images of each other (Fig. 1)

(Continued on p. 634)

* A full listing of bond lengths and angles, of thermal parameters, and Tables of observed and calculated structure factors can be obtained from the authors.

TABLE I
FINAL POSITIONAL PARAMETERS FOR AuFe₃(HC≡NBu¹)(CO)₉(PPh₃)

	<i>x/a</i>	<i>y/b</i>	<i>z/c</i>		<i>x/a</i>	<i>y/b</i>	<i>z/c</i>
Au(1)	3137(1)	1989(1)	10892(1)	Au(2)	7263(1)	2679(1)	5648(1)
Fe(11)	2471(2)	2399(1)	9570(1)	Fe(21)	7271(2)	2583(1)	7068(1)
Fe(12)	1684(2)	1128(1)	10837(1)	Fe(22)	7929(2)	3967(1)	5897(1)
Fe(13)	402(2)	2652(1)	10282(1)	Fe(23)	9131(2)	3074(1)	6936(1)
P(1)	4088(3)	2345(3)	11547(3)	P(2)	6988(3)	2160(3)	4772(2)
N(1)	1905(9)	1341(7)	9693(6)	N(2)	6876(8)	3891(7)	6937(6)
C(11)	804(12)	1618(10)	9946(8)	C(21)	7842(11)	4052(9)	6976(8)
C(12)	2308(12)	652(10)	9254(9)	C(22)	5794(11)	4537(9)	7093(8)
C(13)	1683(15)	-148(13)	9639(11)	C(23)	5418(15)	4239(13)	7989(11)
C(14)	2165(17)	1158(14)	8398(12)	C(24)	4910(15)	4421(12)	6760(11)
C(15)	3566(17)	247(14)	9276(12)	C(25)	5894(15)	5525(12)	6758(10)
C(111)	2503(13)	3369(11)	9706(9)	C(211)	7219(12)	2177(10)	8071(9)
C(112)	2294(18)	3036(16)	8645(14)	C(212)	8067(12)	1573(10)	6957(8)
C(113)	3892(15)	2048(12)	9329(10)	C(213)	6005(13)	2326(10)	7129(9)
C(121)	2876(13)	336(10)	11144(9)	C(221)	7047(12)	4452(10)	5228(9)
C(122)	1115(14)	1584(11)	11585(10)	C(222)	9106(12)	3340(10)	5471(9)
C(123)	878(13)	308(11)	11281(10)	C(223)	8417(13)	4974(11)	5513(9)
C(131)	-52(17)	3431(14)	9481(13)	C(231)	9179(13)	2723(11)	7887(10)
C(132)	339(14)	3459(12)	10701(10)	C(232)	10121(13)	2136(11)	6748(9)
C(133)	-919(16)	2400(13)	10773(11)	C(233)	10075(15)	3763(12)	6685(10)
O(111)	2517(10)	4107(9)	9715(7)	O(211)	7200(8)	1836(7)	8732(6)

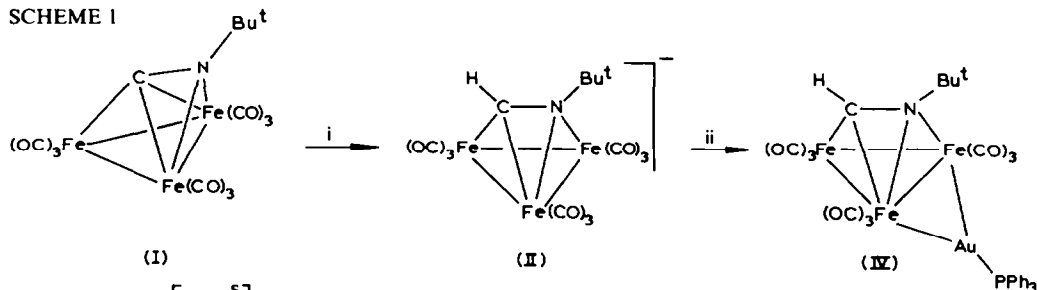
O(112)	2229(13)	3450(11)	7992(10)	O(212)	8579(9)	830(7)	6928(6)
O(113)	4874(12)	1893(9)	9159(8)	O(213)	5195(10)	2055(8)	7246(7)
O(121)	3620(10)	- 242(8)	11381(7)	O(221)	6486(10)	4865(8)	4758(7)
O(122)	727(11)	1744(9)	12177(8)	O(222)	9880(9)	3000(7)	5084(6)
O(123)	290(11)	- 224(8)	11618(7)	O(223)	8730(9)	5672(8)	5235(7)
O(131)	- 371(15)	3963(12)	8917(11)	O(231)	9202(10)	2465(9)	8569(8)
O(132)	281(11)	4042(9)	10939(8)	O(232)	10827(11)	1529(9)	6645(7)
O(133)	- 1734(13)	2166(10)	11145(9)	O(233)	10712(11)	4259(9)	6513(8)
C(141)	3096(7)	2940(6)	12181(5)	C(241)	5559(11)	2062(7)	4927(6)
C(142)	2317(7)	3693(6)	11850(5)	C(242)	5289(7)	1438(7)	4707(6)
C(143)	1459(7)	4107(6)	12320(5)	C(243)	4179(7)	1393(7)	4823(6)
C(144)	1380(7)	3768(6)	13121(5)	C(244)	3339(7)	1972(7)	5159(6)
C(145)	2159(7)	3014(6)	13452(5)	C(245)	3609(7)	2597(7)	5378(6)
C(146)	3017(7)	2600(6)	12982(5)	C(246)	4719(7)	2642(7)	5262(6)
C(151)	4952(8)	1395(6)	12166(5)	C(251)	7316(9)	2882(7)	3764(5)
C(152)	4586(8)	576(6)	12569(5)	C(252)	8031(9)	3468(7)	3590(5)
C(153)	5236(8)	- 158(6)	13041(5)	C(253)	8316(9)	4034(7)	2829(5)
C(154)	6251(8)	- 73(6)	13111(5)	C(254)	7887(9)	4014(7)	2244(5)
C(155)	6616(8)	746(6)	12709(5)	C(255)	7173(9)	3427(7)	2418(5)
C(156)	5966(8)	1480(6)	12237(5)	C(256)	6887(9)	2861(7)	3179(5)
C(161)	5048(7)	3093(6)	10909(5)	C(261)	7807(9)	1041(6)	4833(7)
C(162)	5769(7)	2860(6)	10283(5)	C(262)	8468(9)	842(6)	4177(7)
C(163)	6578(7)	3368(6)	9820(5)	C(263)	9085(9)	- 38(6)	4245(7)
C(164)	6666(7)	4108(6)	9982(5)	C(264)	9042(9)	- 718(6)	4969(7)
C(165)	5945(7)	4340(6)	10608(5)	C(265)	8381(9)	- 519(6)	5626(7)
C(166)	5136(7)	3833(6)	11072(5)	C(266)	7763(9)	360(6)	5558(7)

TABLE 2

SELECTED BOND PARAMETERS FOR $\text{AuFe}_3(\mu_3\text{-HC=NBu}^t)(\text{CO})_9(\text{PPh}_3)$

	Molecule 1	Molecule 2
<i>Bond lengths (Å)</i>		
Au-Fe(1)	2.671(3)	2.659(2)
Au-Fe(2)	2.679(3)	2.717(3)
Fe(1)-Fe(2)	2.662(3)	2.627(2)
Fe(1)-Fe(3)	2.607(3)	2.643(3)
Fe(2)-Fe(3)	2.560(3)	2.574(3)
Au-P	2.286(5)	2.290(5)
Fe(1)-N	1.96(1)	1.97(1)
Fe(2)-N	2.02(1)	2.04(1)
Fe(2)-C(1)	2.08(2)	2.09(2)
Fe(3)-C(1)	1.91(2)	1.94(2)
N-C(1)	1.36(2)	1.37(2)
N-C(2)	1.54(2)	1.51(2)
Fe-CO (average)	1.73	1.74
C-O (average)	1.18	1.19
<i>Bond angles (degrees)</i>		
Fe(1)-Au-Fe(2)	59.7(1)	58.5(1)
P-Au-Fe(1)	147.4(1)	153.8(1)
P-Au-Fe(2)	152.3(1)	147.7(1)
Au-Fe(1)-Fe(2)	60.3(1)	61.9(1)
Au-Fe(1)-Fe(3)	90.1(1)	104.9(1)
Au-Fe(2)-Fe(1)	60.0(1)	59.6(1)
Au-Fe(2)-Fe(3)	90.9(1)	105.1(1)
Fe(1)-Fe(2)-Fe(3)	59.9(1)	61.1(1)
Fe(1)-Fe(3)-Fe(2)	62.2(1)	60.5(1)
Fe(2)-Fe(1)-Fe(3)	58.1(1)	58.5(1)
Fe(1)-N-Fe(2)	83.8(6)	81.9(4)
Fe(2)-C(1)-Fe(3)	79.7(7)	79.4(6)
C(1)-N-C(2)	120.5(15)	119.3(13)
Fe(3)-C(1)-N	116.1(13)	115.2(11)
Fe(1)-N-C(1)	100.7(10)	102.4(8)
Fe(1)-N-C(2)	131.4(8)	133.7(9)
<i>Dihedral angle</i>		
Fe(1)-Au-Fe(2) } Fe(1)-Fe(2)-Fe(3) }	110.9	132.1
<i>Inter-vector angle</i>		
C(1)-N/Fe(1)-Fe(3)	10.8	8.5

SCHEME 1



Reagents : i, $\text{K}[\text{HBBu}_3^{\text{S}}]$; ii, $\text{AuCl}(\text{PPh}_3)$

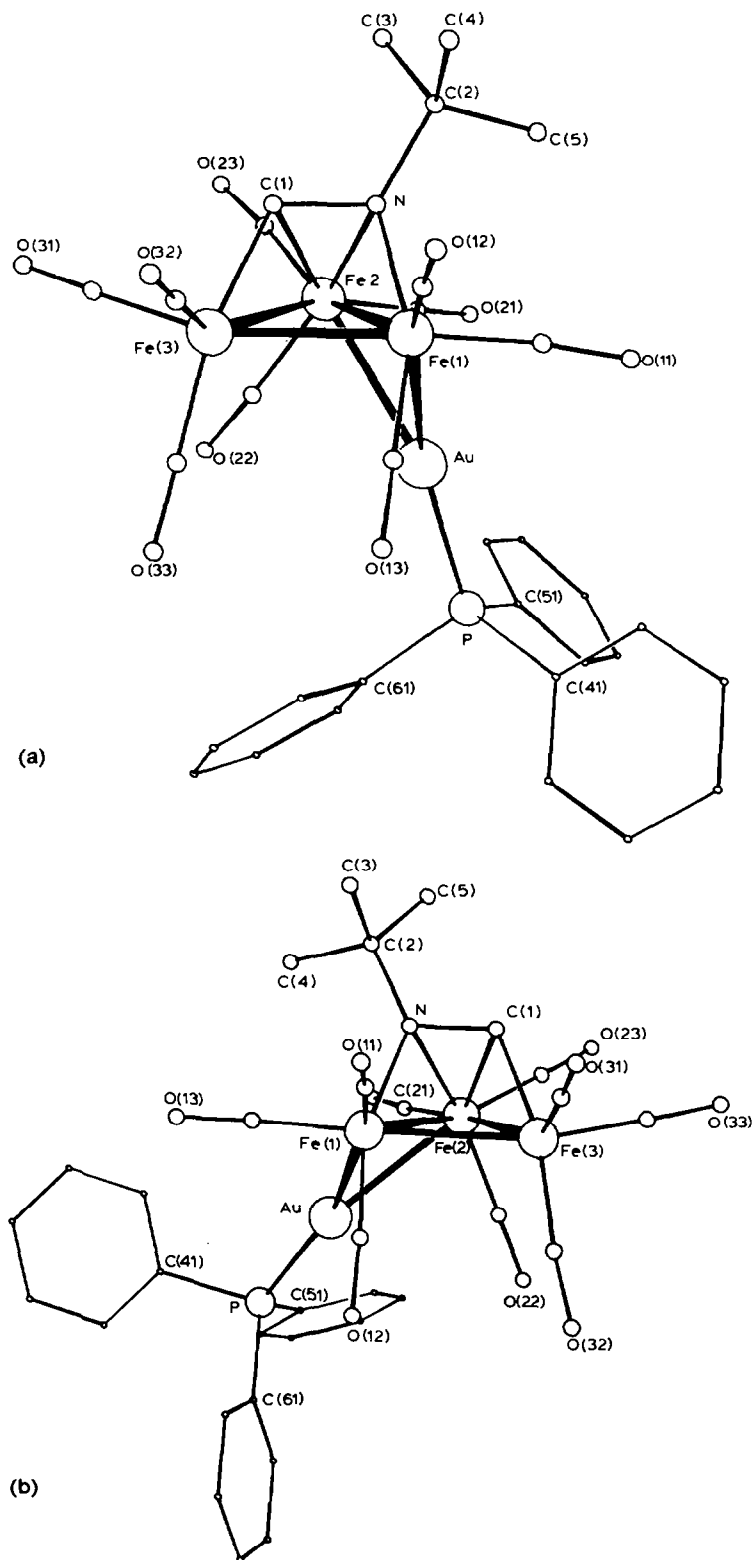


Fig. 1. Perspective views of the two independent molecules of $\text{AuFe}_3(\mu_3\text{-HC=NBu}^t)(\text{CO})_9(\text{PPh}_3)$: (a) Molecule 1, (b) Molecule 2.

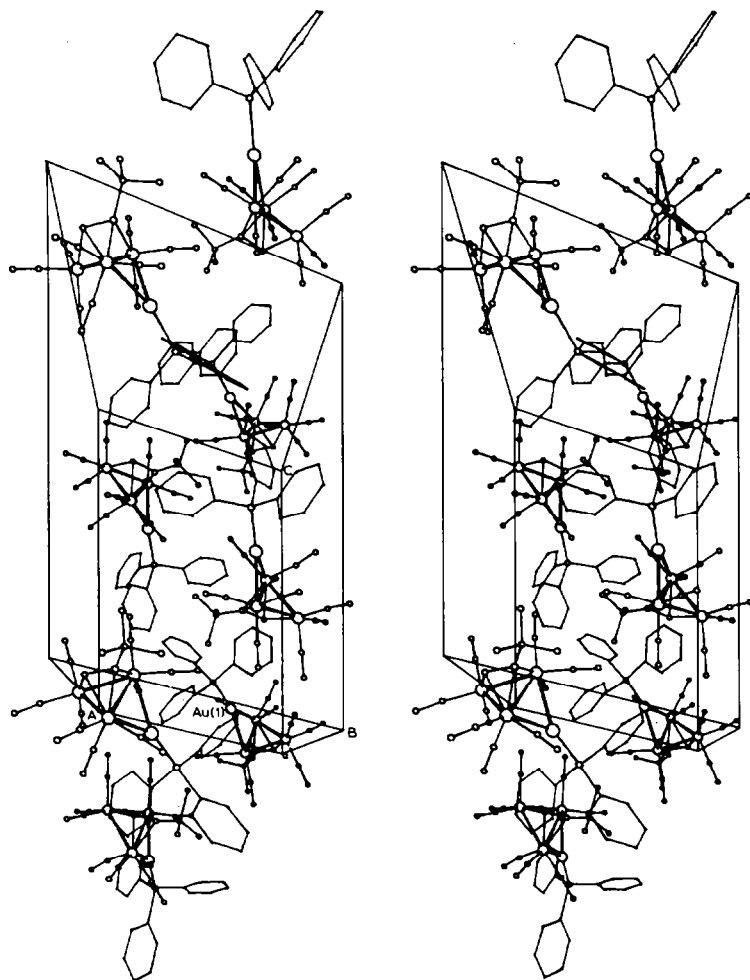


Fig. 2. The packing of $\text{AuFe}_3(\mu_3\text{-HC=Nbu})(\text{CO})_9(\text{PPh}_3)$ in the unit cell viewed approximately along the b axis.

although there are significant differences in bond parameters (*vide infra*). The $\text{Au}(\text{PPh}_3)$ group bridges the $\text{Fe}(1)\text{-Fe}(2)$ edge of the Fe_3 triangle and is directed to the opposite side of the triangle to that occupied by the $(\mu_3\text{-HC=Nbu})$ ligand. This constitutes the first example of a “butterfly” cluster in the AuFe_3 system similar to the AuRu_3 and AuOs_3 species already known.

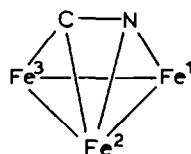
In retrospect it is not surprising that the $\text{Au}(\text{PR}_3)$ group bridges an Fe-Fe edge rather than capping the Fe_2CN face of the cluster precursor. In this respect the situation is similar to that found in III. Recent discussions [2,4] have emphasised that $\text{Au}(\text{PR}_3)$ is isolobal with H, in that it behaves as though it is sp hybridised, with one lobe available for cluster bonding. Minor interactions involving the remaining p orbitals are probable in some situations, especially where there are two or more gold atoms in adjacent sites in the cluster [7,8,22]. The theoretical parallel between H and $\text{Au}(\text{PR}_3)$ groups is supported by a number of examples of clusters which have

Au(PR₃) groups in sites occupied by H in the hydride analogues; examples containing these ligands in either doubly or triply bridging sites have been studied [2,8,22,23].

However, there is no obvious reason why the gold atom bridges Fe(1)–Fe(2), when by analogy with the molecule HFe₃(μ₃-HN=CMe)(CO)₉ (V) [15], it would have been expected to bridge the Fe(1)–Fe(3) bond. An electronic preference seems unlikely since the observed arrangement leads to an unsymmetrical electron distribution, normal electron book-keeping giving 18, 19 and 17-electron configurations for Fe(1), Fe(2) and Fe(3), respectively, whereas in the expected Fe(1)–Au–Fe(3) isomer, each iron atom attains the normal 18-electron configuration. Similarly, there seem to be no steric grounds for avoiding an Fe(1)–Fe(3) bridge since each iron atom has three equivalently disposed terminal CO ligands, and the μ₃-HC=NBu^t group is too far removed to have any direct steric influence on the Au(PPh₃) unit. The possibility that the μ₃-HC=NBu^t group constrains the Fe(1)–Fe(3) bond to a length incompatible with a μ-Au(PR₃) unit can also be excluded since the observed Fe(1)–Fe(2) and Fe(1)–Fe(3) separations are quite similar (see also below).

It has been shown that HFe₃(μ₃-HC=NPrⁱ)(CO)₉ is fluxional, involving movement of both the H and HC=NPrⁱ ligands [16]. It may be that similar fluxionality occurs for IV and the structure observed is one of several interconverting forms frozen in the solid. However, it is to be noted that there are two independent molecules of IV in the asymmetric unit of the crystal and both have the same basic structure. Since each has a different crystal environment it would be quite possible for each to have the Au in different bridging positions if crystal packing forces alone were responsible for choosing one among several isomers.

Comparisons of the structure of IV with that of V reveal similarities in the Fe₃(μ₃-ligand) geometries. However, inspection of the Fe–CO distances (1.73,

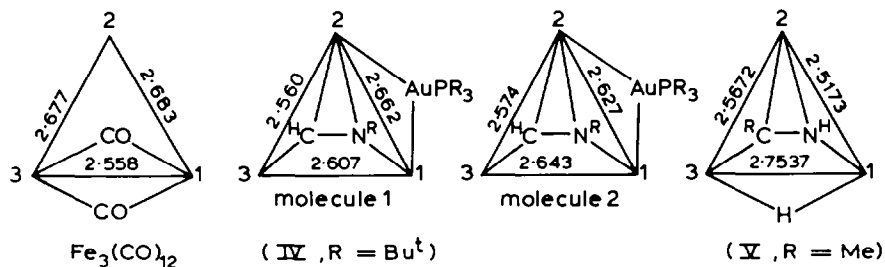


Atom separations (Å)

	IV		V
Fe(1)–N	1.96(1)	1.97(1)	1.931(2)
Fe(2)–N	2.02(1)	2.04(1)	2.001(2)
Fe(2)–C	2.08(2)	2.09(2)	2.096(2)
Fe(3)–C	1.91(2)	1.94(2)	1.933(2)
C–N	1.36(2)	1.37(2)	1.344(2)

1.74(av) for IV, 1.800 Å (av) for V) suggests that in the former, the electron density on the iron atoms is greater and back-bonding is more efficient. The HC=NBu^t ligand triply bridges the Fe₃ triangle and is bonded in a 2σ (Fe(1)–N and Fe(3)–C(1)) + π (to Fe(2)) fashion. As expected the C(1)–N bond length in the μ₃-ligand is intermediate between those of C–N single and C=N double bonds, and somewhat longer than that in V. The ligand is formally a HC=NBu^t group, and the C=N bond lengthening is undoubtedly the result of π-bonding to Fe(2).

There are several points of interest in the geometry of the AuFe₃ metal cluster. A comparison of the Fe–Fe bond lengths in the two molecules of IV, in V and in Fe₃(CO)₁₂ [24] is instructive, and the diagram summarises the available data. If the non-bridged distance in the latter (2.680 Å av) is taken as a starting point, it can be seen that the C-bridged Fe(2)–Fe(3) distances in both IV and V are ca. 0.11 Å shorter. In IV, where Fe(1)–Fe(3) is bridged by the HC=NBu^t ligand, the separation



has decreased by ca. 0.055 Å (compared with Fe(1)–Fe(2) in $\text{Fe}_3(\text{CO})_{12}$). In V, where this bond is also bridged by the hydrogen (which was located in the structural study [15]), the distance increases by 0.074 Å to 2.754 Å, so that the bond-lengthening effect of the $\mu\text{-H}$ ligand can be estimated at $0.074 + 0.055 = 0.129$ Å. In V also, the N-bridged Fe(1)–Fe(2) bond is 0.163 Å shorter than the unbridged Fe–Fe bond in $\text{Fe}_3(\text{CO})_{12}$, while in IV, where this bond is the hinge of the AuFe_3 butterfly, the separation is 2.645 Å, or about 0.127 Å longer than found in V. This difference is virtually identical to that which would be expected if the bond lengthening effects of these ligands are additive, and if the effect of a $\mu\text{-H}$ atom is the same as that of a $\mu\text{-Au}(\text{PR}_3)$ group. In the above discussion we have used average values of the Fe–Fe separations found in the two independent molecules of IV; although these are significantly different if taken individually, we note that the average values are closely similar in IV and V.

These results suggest that local differences in electron density in the cluster can be compensated by complementary expansion and contraction of individual metal–metal bonds. In addition, the apparent additivity of these elongation or shortening influences of the bridging ligands is consistent with the Fe(1)–Fe(3) separation in V being the combined result of the two bridging ligands, rather than the second ligand ($\text{MeC}=\text{NH}$) masking the usual bond-lengthening effect of a $\mu\text{-H}$ ligand, as originally suggested [15]. This conclusion rests on the effect of a $\mu\text{-Au}(\text{PPh}_3)$ group being similar to that of the $\mu\text{-H}$ atom; further examples are needed before the generality of this observation is proved.

A further point of interest in the structure of IV relates to the dihedral angle between the AuFe_2 and Fe_3 planes. This ‘hinge’ angle differs markedly in the two independent molecules, having values of 110.9° and 132.1°. This deformation has little effect on the rest of the molecule except for the carbonyl ligands on Fe(2) which are twisted by ca. 12°. As the dihedral angle increases, the Fe(1)–Fe(3) separation also increases by ca. 0.04 Å, while the Fe(1)–Fe(2) separation decreases by a similar amount. The Au–P vector intersects the Fe_3 plane along the Fe(1)–Fe(2) vector in molecule 2, but somewhat outside the Fe_3 triangle in molecule 1 (Fig. 3). A possible explanation is that the opening of the dihedral angle leads to less efficient overlap of metal orbitals between Fe(1) and Fe(3); the concomitant movement of CO groups maps the direction of orbitals pseudotrans to the equatorial CO. In both molecules, the arrangement of CO groups differs significantly from that in V, where the $\mu\text{-H}$ is almost coplanar with the Fe_3 triangle. The implications of these observations await comparative structural analyses of other $\mu\text{-H}/\mu\text{-Au}(\text{PR}_3)$ pairs.

There are several M_4 “butterfly” clusters known, with varying dihedral angles between the wings. A recent report [25] has attempted to relate the dihedral angle to the cluster electron-count, and suggests that the more electron-rich species may open

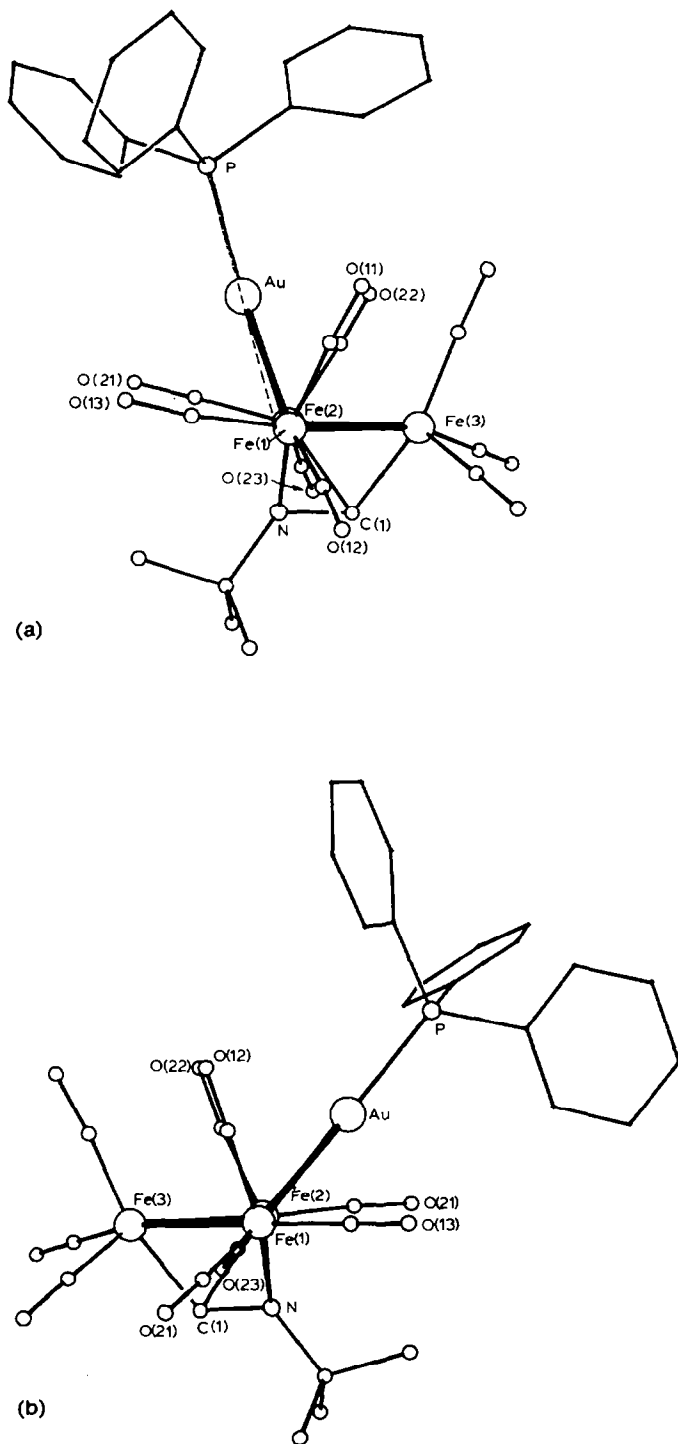


Fig. 3. Diagrams of (a) Molecule 1 and (b) Molecule 2 of $\text{AuFe}_3(\mu_3\text{-HC}\equiv\text{NBu}')(\text{CO})_9(\text{PPh}_3)$, looking down the $\text{Fe}(1)\text{-Fe}(2)$ bond, showing the intercepts of the Au-P vectors with the Fe_3 planes.

out to become nearly flat. The difference of more than 20°, and concomitant increase in separation of the wing-tip atoms from 3.74 Å (molecule 1) to 4.20 Å (molecule 2), found in the present study of IV can only be attributed to crystal-packing effects, and there is no indication from the lattice packing (Fig. 2) that these forces are at all severe. It follows that deformation of the wings is a low energy process, so that caution should be exercised when comparing “butterfly” angles from solid state measurements. Indeed, the system seems to be so flexible that it is likely that in solution, the “butterfly” wings will flap!

Acknowledgements

We thank the Australian Research Grants Committee for financial support and the University of Waikato for providing study leave (to B.K.N.). We are grateful to Dr. M.R. Snow for the use of X-ray facilities.

References

- 1 C.E. Coffey, J. Lewis and R.S. Nyholm, *J. Chem. Soc.*, (1964) 1741.
- 2 J.W. Lauher and K. Wald, *J. Am. Chem. Soc.*, 103 (1981) 7648.
- 3 B.F.G. Johnson, D. Kaner, J. Lewis and P.R. Raithby, *J. Chem. Soc., Chem. Commun.*, (1981) 953; *J. Organometal. Chem.*, 215 (1981) C33.
- 4 D.G. Evans and D.M.P. Mingos, *J. Organometal. Chem.*, 232 (1982) 171.
- 5 J.E. Ellis, *J. Am. Chem. Soc.*, 103 (1981) 6106.
- 6 B.F.G. Johnson, D.A. Kaner, J. Lewis, P.R. Raithby and M.J. Taylor, *Polyhedron*, 1 (1982) 105.
- 7 L.W. Bateman, M. Green, J.A.K. Howard, K.A. Mead, R.M. Mills, I.D. Salter, F.G.A. Stone and P. Woodward, *J. Chem. Soc., Chem. Commun.*, (1982) 773.
- 8 M.I. Bruce and B.K. Nicholson, *J. Chem. Soc., Chem. Commun.*, (1982) 1141.
- 9 A.N. Nesmeyanov, E.G. Perevalova, Y.T. Struchkov, M.Y. Antipin, K.I. Grandberg and V.P. Dyadchenko, *J. Organometal. Chem.*, 201 (1980) 343.
- 10 M.I. Bruce, E. Horn, O. bin Shawkataly and M.R. Snow, unpublished results.
- 11 M.I. Bruce, T.W. Hambley and B.K. Nicholson, *J. Chem. Soc., Chem. Commun.*, (1982) 353.
- 12 M.I. Bruce and R.C. Wallis, *J. Organometal. Chem.*, 164 (1979) C6; *Aust. J. Chem.*, 35 (1982) 709.
- 13 C.C. Yin and A.J. Deeming, *J. Organometal. Chem.*, 133 (1977) 123; R.D. Adams and N.M. Golembeski, *J. Am. Chem. Soc.*, 100 (1978) 4622; 101 (1979) 2579.
- 14 M.A. Andrews and H.D. Kesz, *J. Am. Chem. Soc.*, 101 (1979) 7238, 7255.
- 15 M.A. Andrews, G. van Buskirk, C.B. Knobler and H.D. Kesz, *J. Am. Chem. Soc.*, 101 (1979) 7245.
- 16 J.A.S. Howell and P. Mathur, *J. Chem. Soc., Dalton Trans.*, (1982) 43.
- 17 B.E.R. Schilling and R. Hoffmann, *J. Am. Chem. Soc.*, 101 (1979) 3456.
- 18 K. Wade, *Advan. Inorg. Chem. Radiochem.*, 18 (1976) 1.
- 19 B.F.G. Johnson, D.A. Kaner, J. Lewis, P.R. Raithby and M.J. Rosales, *J. Organometal. Chem.*, 231 (1982) C59.
- 20 M.I. Bruce and B.K. Nicholson, *J. Chem. Soc., Dalton Trans.*, submitted.
- 21 SUSCAD, Data reduction programme for the CAD4 diffractometer, University of Sydney, 1976; ABSORB, Programme for correcting for absorption effects, University of Sydney, 1976; SHELX-76, Programme for crystal structure determination, G. Sheldrick, University of Cambridge, 1976.
- 22 J. Lewis and B.F.G. Johnson, *Pure Appl. Chem.*, 54 (1982) 97; B.F.G. Johnson, D.A. Kaner, J. Lewis, P.R. Raithby and M.J. Taylor, *J. Chem. Soc., Chem. Commun.*, (1982) 314.
- 23 M.J. Mays, P.R. Raithby, P.L. Taylor and K. Henrick, *J. Organometal. Chem.*, 224 (1982) C45.
- 24 F.A. Cotton and J.M. Troup, *J. Am. Chem. Soc.*, 98 (1976) 4155.
- 25 A.J. Carty, S.A. MacLaughlin, J.V. Wagner and N.J. Taylor, *Organometallics*, 1 (1982) 1013.
- 26 M.I. Bruce, B.K. Nicholson and M.L. Williams, *J. Organometal. Chem.*, 243 (1983) 69.